MINIMIZATION OF GRID ORIENTATION EFFECTS BY USING ENO AND TVD SCHEMES IN RESERVOIR SIMULATION USING NON-ORTHOGONAL BOUNDARY-FITTED COORDINATES

A.O. Czesnat
C.R. Maliska
A.F.C Silva
R.M. Lucianetti
SINMEC – Laboratório de Simulação Numérica em Mecânica dos Fluidos e Transferência de Calor
Departamento de Engenharia Mecânica
Universidade Federal de Santa Catarina
88040-900 – Florianópolis – SC – Brasil

Abstract. The solution of the displacement front is one of the toughest problems in reservoir simulation, since its accuracy depends strongly on the approximation scheme used for the convective terms of the governing equations. The scheme normally used is the UDS (Upstream Differencing Scheme) that stabilizes the numerical solution, but introduces high levels of numerical diffusion. The numerical diffusion provokes two important manifestations. One is the smearing of the front, which can cause wrong forecasts of the breakthrough. The other one is the distortion of the displacement front, the well-known grid orientation effect. High-resolution methods, like TVD (Total Variation Diminishing) and ENO (Essentially Non-Oscillatory), are able to reduce the numerical diffusion. Specialized literature in reservoir simulation shows how to implement TVD schemes in a cartesian and boundary-fitted coordinates. On the other hand, ENO scheme was introduced in reservoir simulation only for cartesian grids. This paper suggests an ENO scheme to be used in reservoir simulation with boundary-fitted coordinates. The performance of numerical methods, like UDS, TVD and ENO, is analyzed for a reservoir engineering problem and comparisons are made with a refined grid UDS solution.

Key words: Grid orientation effect, ENO, Boundary fitted coordinates

1. INTRODUCTION

The governing equations of the multiphase flow in porous media are obtained performing a mass balance for each component. Pressure and saturation or mass fractions, of each component, are the unknowns. In this equation system, saturation behaves predominantly hyperbolic while pressure shows a parabolic behavior. Therefore, one expects, generally, a continuous pressure distribution in the reservoir while saturation can present discontinuities.

Therefore, the hyperbolic nature of saturation is the main concern when concerning the interpolation schemes.

The solution of the displacement front is a one of the toughest problems in reservoir simulation and its accuracy depends strongly on the approximation scheme used for the convective terms of the governing equations. The scheme normally used is the UDS, which stabilizes the numerical solution and always gives physical solutions, but introduces high levels of numerical diffusion. Hence, this method excessively smears the front. The use of higher-order schemes brings spurious oscillation in the computed solution, so, they are not a reliable alternative. It is important to note that the difficulty is not restricted to petroleum reservoir simulation, but to all the conservation laws systems with dominant convection.

The numerical diffusion has two important consequences. One is the smearing of the front, which can cause wrong forecasts of the breakthrough. The other one is the distortion of the displacement front, the so-called grid orientation effect, that is a multidimensional effect of the numerical diffusion. One can say that the front smearing is strongly related to the magnitude of the numerical diffusion and the grid orientation effect to the magnitude of the numerical diffusion in each direction. It is worth noting that both effects depend on the numerical diffusion magnitude, consequently, its minimization results in the reduction of both effects.

Following these ideas, the main concern of this paper is to apply high-resolution methods, like TVD and ENO, to the solution of displacement processes to allow accurate resolution of the fronts and minimization of the numerical diffusion, and, therefore, reduction of the grid orientation effect. The main contribution of this paper is the implementation of an ENO scheme for non-orthogonal boundary-fitted grids.

2. LITERATURE REVIEW

Todd *et al*. (1972) raised the so-called grid orientation effect. They studied two five-spot grid systems, diagonal and parallel, and demonstrated that the predicted recovery performance depends on the grid used. They proposed a two-point upstream scheme to reduce grid orientation effect. The method is second-order in space and diminishes the numerical diffusion's effects, however, in some cases there are spurious oscillations.

Yanosik and McCracken (1976) observed that the probably grid orientation effect was caused by not accounting for the diagonal flow by the five-point finite-difference formulation. They presented a nine-point formulation that accounts for this flow. The authors showed many results for unfavorable mobility-ratios, getting almost identical results for both diagonal and parallel grids. One can conclude, observing these results, that the numerical diffusion was absent in these simulations, but it is not true, since formulations bring a truncate errors homogenization, and, consequently, obtain solutions with equal quantities of numerical diffusion.

Harten (1983) inspired by Glim and Lax (1970), who had shown that the total variation of the solution of a scalar one-dimensional conservation law can not increase, introduced the total variation of a discrete function as a measure of its oscillatory nature. This led to the formulation of the Total Variation Diminishing (TVD) schemes and the term quickly became synonymous for high-resolution schemes.

Taggart and Pinczewski (1987), using finite differencing, developed uniform second and third-order schemes to solve flows in porous media. They showed that the use of high-order schemes bring better solution of the fronts and, in some cases, minimize the grid orientation effect. Nevertheless, it was necessary to add physical dispersion in the model.

Harten and Osher (1987) and Harten *et al*. (1987) reexamined non-oscillatory interpolation theory and developed the ENO schemes. After that, Shu and Osher (1988a, 1988b) developed an efficient and simpler manner to implement ENO schemes.

Rubin and Blunt (1991) introduced a TVD scheme simple to apply to both IMPES Black-Oil models and fully implicit Black-Oil models. It was obtained using a first-order time discretization version of the second-order TVD flux limited Lax-Wendroff scheme.

Pinto *et al*. (1991) applied TVD schemes to non-uniform cartesian grids directly in the relative permeability. It was shown that it produced better results than when applied in the total flux terms as Rubin and Blunt (1991) proposed.

Chen *et al*. (1991) obtained the minimization of the grid orientation effect through the use of second-order TVD and third-order ENO in five-spot problems. The authors concluded that the use of an ENO scheme reduces the grid orientation effect relative to the first order method, UDS. They also stressed that high-resolution methods accurately resolve displacement fronts and therefore yield much more reliable solutions than do first-order methods. In addition, using high-resolution method, many fewer grid blocks can be used to achieve the same accuracy as a first-order method.

Maliska *et al*. (1993) and Cunha *et al*. (1994) obtained results very close to the Yanosik and McCracken's formulation, using boundary-fitted coordinates aligned to the flow and UDS scheme. The authors pointed out that it is not always possible to find a curvilinear grid which fits the flow direction and, therefore, the use of boundary-fitted grids is not a remedy to eliminate the numerical diffusion.

Mota and Maliska (1994) extended the Rubin and Blunt TVD to boundary-fitted coordinates, applying the scheme to the relative permeability. They concluded that, in many cases, the results obtained with TVD are equivalent to the UDS results with three or more times the number of grid nodes.

3. PROBLEM FORMULATION

3.1 Mathematical model

The problem under consideration is the two-phase oil and water problem. The mass balances for each component, oil and water for two-phase problem gives

$$\frac{\partial}{\partial t}\left[\phi\rho^m Z^w\right] = \nabla.\left[\lambda^w \nabla\Phi^w\right] - m^w \tag{1}$$

$$\frac{\partial}{\partial t}\left[\phi\rho^m Z^o\right] = \nabla.\left[\lambda^o \nabla\Phi^o\right] - m^o \tag{2}$$

where's ϕ, λ^p, Z^i, Φ^p, ρ^m are the porosity, permeability of phase p, mass fraction of the i component, phase p potential and average density, respectively.

Inspecting Eq. (1) and Eq. (2) one can see that the mass fractions Z^w, Z^o and the phase potentials are unknowns. The phase potentials can be related to the oil pressure by capillary pressures, consequently, the unknowns of the equation system become the mass fractions and the oil pressure. So, there are two equations and three unknowns, requiring a closure equation. In this case, the global mass conservation, water plus oil, is invoked. This is called the constraint equation and is expressed by

$$Z^o + Z^w = 1 \tag{3}$$

In spite of having a well-posed problem, Eq. (1) to Eq. (3) do not form an appropriate equation system to be solved by iterative methods. To obtain Z^w, Z^o, in such a way that Eq. (3) is conserved, would require the creation of a correction equation to advance one of the mass fractions based on the error of the global mass conservation. Therefore, it is preferable to satisfy Eq. (3) by adding up Eq. (1) to Eq. (2) and discarding the mass conservation for the oil component, Eq. (2). Using this procedure, one finds the global mass conservation equation, given by

$$\frac{\partial}{\partial t}\left[\phi\rho^m\right] = \nabla.\left[\lambda^w\nabla\Phi^w + \lambda^o\nabla\Phi^o\right] - m^w - m^o \tag{4}$$

The corresponding equation system to be solved is, therefore, formed by Eq. (1), Eq. (3) and Eq. (4). In all boundaries, it is prescribed no-flow boundary condition.

In order to complete the mathematical model, one need to define the initial conditions, i.e., the initial pressure and saturation or mass fraction fields. A more detailed explanation of the mathematical model, used in the present work can be seen in Maliska *et al*. (1997).

3.2 Numerical model

The equation system is solved using the fully implicit formulation with Newton's method in a generalized curvilinear coordinated framework. The conservation equations are transformed to the new coordinated system, (ξ, η, γ), and then integrated in a regular domain, as described in Maliska (1995). To illustrate, the transformed equation for the water component, Eq. (1), is taken as an example and written below as

$$\frac{1}{J}\frac{\partial}{\partial t}\left(\phi\rho^m z^w\right) + \frac{m^w}{J} = \frac{\partial}{\partial\xi}\left[D_{11}^w\frac{\partial\Phi^w}{\partial\xi} + D_{12}^w\frac{\partial\Phi^w}{\partial\eta} + D_{13}^w\frac{\partial\Phi^w}{\partial\gamma}\right] +$$
$$\frac{\partial}{\partial\eta}\left[D_{21}^w\frac{\partial\Phi^w}{\partial\xi} + D_{22}^w\frac{\partial\Phi^w}{\partial\eta} + D_{23}^w\frac{\partial\Phi^w}{\partial\gamma}\right] + \frac{\partial}{\partial\gamma}\left[D_{31}^w\frac{\partial\Phi^w}{\partial\xi} + D_{32}^w\frac{\partial\Phi^w}{\partial\eta} + D_{33}^w\frac{\partial\Phi^w}{\partial\gamma}\right] \tag{5}$$

The equation for the pressure is similar and is not presented here. The finite-volume method, which consists in integrating the conservation equations in their divergence form, is used. Integration of Eq. (5) in time and in space results

$$\frac{1}{J}\left[\left(\phi\rho^m Z^w\right)_p - \left(\phi\rho^m Z^w\right)_p^o\right]\Delta V + \frac{m^w}{J}\Delta V\Delta t =$$
$$\left[D_{11}^w\frac{\partial\Phi^w}{\partial\xi} + D_{12}^w\frac{\partial\Phi^w}{\partial\eta} + D_{13}^w\frac{\partial\Phi^w}{\partial\gamma}\right]_e \Delta\eta\Delta\gamma\Delta t - \left[D_{11}^w\frac{\partial\Phi^w}{\partial\xi} + D_{12}^w\frac{\partial\Phi^w}{\partial\eta} + D_{13}^w\frac{\partial\Phi^w}{\partial\gamma}\right]_w \Delta\eta\Delta\gamma\Delta t +$$
$$\left[D_{21}^w\frac{\partial\Phi^w}{\partial\xi} + D_{22}^w\frac{\partial\Phi^w}{\partial\eta} + D_{23}^w\frac{\partial\Phi^w}{\partial\gamma}\right]_n \Delta\xi\Delta\gamma\Delta t - \left[D_{21}^w\frac{\partial\Phi^w}{\partial\xi} + D_{22}^w\frac{\partial\Phi^w}{\partial\eta} + D_{23}^w\frac{\partial\Phi^w}{\partial\gamma}\right]_s \Delta\xi\Delta\gamma\Delta t + \tag{6}$$
$$\left[D_{31}^w\frac{\partial\Phi^w}{\partial\xi} + D_{32}^w\frac{\partial\Phi^w}{\partial\eta} + D_{33}^w\frac{\partial\Phi^w}{\partial\gamma}\right]_t \Delta\xi\Delta\eta\Delta t - \left[D_{31}^w\frac{\partial\Phi^w}{\partial\xi} + D_{32}^w\frac{\partial\Phi^w}{\partial\eta} + D_{33}^w\frac{\partial\Phi^w}{\partial\gamma}\right]_b \Delta\xi\Delta\eta\Delta t$$

where D_{ij} is given by

$$D_{ij}^{p} = \frac{\lambda^{p}}{J}\left[\frac{\partial x^{i}}{\partial x}\frac{\partial x^{j}}{\partial x} + \frac{\partial x^{i}}{\partial y}\frac{\partial x^{j}}{\partial y} + \frac{\partial x^{i}}{\partial z}\frac{\partial x^{j}}{\partial z}\right] \qquad (7)$$

with i, j = 1, 2 or 3 and x^{1}, x^{2} e x^{3} are ξ, η and γ, respectively.

Note that the D_{ij} terms, Eq. (7), must be calculated in each face of the control volume. Hence, the mobilities, stored at the center of the volume, need to be interpolated. The quality of the approximation scheme used for the face evaluations of the mobilities strongly influences the displacement front solution accuracy. Complete explanation of the numerical model used in the present work can be seen in Maliska *et al.* (1997).

4. PROPOSED SCHEME

In this section the Shu and Osher's ENO scheme is presented and an ENO scheme to be used in reservoir simulation with boundary-fitted coordinates is advanced. The UDS and TVD implementation schemes are not presented here. For details see Czesnat *et al.* (1998).

ENO schemes are essentially, but not entirely, non-oscillatory and can yield solutions with oscillations of magnitude O[Δx^{r}], where r is the order of the method. These oscillations, from a practical point of view, in no way degrade the solution.

Shu and Osher (1988a, 1988b) suggested an efficient and much easier way to construct ENO schemes than suggested by Harten and Osher (1987) and Harten *et al.* (1987). This methodology is based on numerical fluxes rather than cell-averages and uses the Runge-Kutta method for time discretization. Since neither the reconstruction step nor the Lax-Wendroff time discretization methodologies are necessary, the multidimensional implementation becomes easier.

Summarizing, this scheme uses the interpolation of two polynomials in the upstream and downstream face to evaluate the convective flux. Therefore, to obtain a smooth approximation, the polynomials are compared and the quantity with the smaller absolute value is used. These polynomials are built through divided differences. For example, the first two divided differences of a function f are

$$f[S_{i}] = f(S_{i}) \qquad (8)$$

$$f[S_{i}, S_{i+1}] = \frac{f(S_{i+1}) - f(S_{i})}{x_{i+1} - x_{i}} \qquad (9)$$

Cartesian ENO scheme. Consider a conservation law where F expresses the convective flux and is a function of S. In the east face, one has

$$F_{e} = \frac{dQ(x)}{dx}\bigg|_{e} \qquad (10)$$

where Q is a function that represents the integral of the flux.

Polynomials are used to construct the function Q and they approximate this function in some order using an adaptive stencil. Assuming that $\partial F/\partial S > 0$, the first-order representation of Q, Q_{1}, is

$$Q_{1}(x) = F[S_{P}] \cdot (x - x_{w}) \qquad (11)$$

To compute the second-order contribution to Q, two divided differences designated a_2 and b_2 must be formed as follows:

$$a_2 = \frac{1}{2} F[S_P, S_E] \quad and \quad b_2 = \frac{1}{2} F[S_W, S_P] \tag{12}$$

The magnitude of a_2 and b_2 are then compared and the quantity of smaller absolute value is chosen to represent Q_2. Assuming $|b_2| < |a_2|$, Q_2 is given by

$$Q_2(x) = Q_1(x) + b_2 \cdot (x - x_w) \cdot (x - x_e) \tag{13}$$

To obtain the third order, two additional divided differences must be formed. The differences formed depend on the choice of a_2 or b_2 in Eq. (13). For $|b_2| < |a_2|$ the differences of interest are

$$a_3 = \frac{1}{3} F[S_W, S_P, S_E] \quad and \quad b_3 = \frac{1}{3} F[S_{WW}, S_{WP}, S_P] \tag{14}$$

Like before, the quantity with smaller magnitude is used to approximate Q. For $|b_3| < |a_3|$, Q_3 is

$$Q_3(x) = Q_2(x) + b_3 \cdot (x - x_{ww}) \cdot (x - x_w) \cdot (x - x_e) \tag{15}$$

This scheme is third-order accurate in smooth regions, except at the zeros of flux derivatives, where it may degenerate to second order. In discontinuous regions, the ENO, like TVD, applies the UDS interpolation. It is worth noting that the ENO and TVD schemes can be seen as an UDS approximation by adding anti-diffusive terms. In addition, one can observe that the first two terms of the ENO scheme are equal to the TVD with the minmod limiting function.

Boundary-fitted coordinates ENO scheme. The proposed scheme guarantees two important characteristics. The first one is that the generalized ENO scheme recovers the original, presented in the previous section, when applied to a cartesian grid. The second one is to obtain a generalized ENO scheme, which converts onto a generalized TVD when only the first two terms are used, as explained in Mota and Maliska (1994) and Czesnat *et al.* (1998).

The transformation of the scheme is based on the transformation of the divided difference table. The divided difference with one argument transformed remains the same, but the one with two arguments, refer to Eq. (9), can be recognized as the first derivative second-order approximation, in this case in the x direction

$$\left. \frac{\partial F}{\partial x} \right|_e = F[S_P, S_E] + O(\Delta x^2) \tag{16}$$

So, the transformation to the generalized system is

$$F[S_P, S_E] \Rightarrow \left(\vec{\nabla} F \cdot \hat{e}_\xi \right)_e \tag{17}$$

where $\Rightarrow$ represents the transformation and $\hat{e}_\xi$ is the normalized ξ covariant base vector, given by

$$\hat{e}_\xi = \frac{\vec{e}_\xi}{|\vec{e}_\xi|} = \frac{\partial x}{\partial \xi}\hat{i} + \frac{\partial y}{\partial \xi}\hat{j} + \frac{\partial z}{\partial \xi}\hat{k} \bigg/ \sqrt{\left(\frac{\partial x}{\partial \xi}\right)^2 + \left(\frac{\partial y}{\partial \xi}\right)^2 + \left(\frac{\partial z}{\partial \xi}\right)^2} \tag{18}$$

In order to attend the second characteristic, the Eq. (17) must be modified to

$$F[S_P, S_E] \Rightarrow \vec{\nabla}F_e \cdot \hat{e}_{\xi\,upstream-volume} \tag{19}$$

where $\hat{e}_\xi$ is evaluated in the volume immediately upstream of the flow direction on the interpolated face.

After the above definition, it is assumed that the three argument divided difference can be given by

$$F[S_P, S_E, S_{EE}] = \frac{F[S_E, S_{EE}] - F[S_P, S_E]}{\sum\limits_{k=P}^{E} \left(\sqrt{g_{11}}\right)_{k+1/2}} \tag{20}$$

where g_{11} is the component 1x1 of the metric tensor, given by

$$g_{11} = \frac{\partial x}{\partial \xi}\frac{\partial x}{\partial \xi} + \frac{\partial y}{\partial \xi}\frac{\partial y}{\partial \xi} + \frac{\partial z}{\partial \xi}\frac{\partial z}{\partial \xi} \tag{21}$$

Now it is possible to evaluate F in a generalized form. For instance, on the east face, F is approximate by

$$F_e = Q(x)_e \tag{22}$$

Again, polynomials are used to construct the function Q. Assuming that $\partial F/\partial S > 0$, the first-order representation of Q, Q_1, is

$$Q_1(x) = F[S_P] \tag{23}$$

To compute the second-order contribution to Q, one can use a_2 and b_2 defined by Eq. (12), but now Eq. (19) must be applied.

The magnitude of a_2 and b_2 are then compared and the quantity of smaller absolute value is chosen to represent Q_2. Assuming $|b_2| < |a_2|$, Q_2 is

$$Q_2(x) = Q_1(x) + b_2 \cdot \left(\sqrt{g_{11}}\right)_P \tag{24}$$

For $|b_2| < |a_2|$ using a_3 and b_3 defined by Eq. (14), one can obtain Q_3 by applying Eq. (20). Again assuming $|b_3| < |a_3|$, Q_3 is

$$Q_3(x) = Q_2(x) + b_3 \cdot \left(\sqrt{g_{11}}\right)_P \cdot \left(\left(\sqrt{g_{11}}\right)_P + \left(\sqrt{g_{11}}\right)_W\right) \tag{25}$$

Boundary-fitted coordinates ENO scheme applied to petroleum equations. The generalized ENO scheme is applied to the mobilities of the governing equations, Eq. (1) and Eq. (4). It is worth noting that this methodology could be applied to the gas equation too, and so, can be used in three-phase reservoir problems.

To evaluate the mobility, one must use the Eq. (22) to (25), replacing F by λ.

5. RESULTS

In order to investigate the grid orientation effect, Hegre *et al.* (1986) create a problem with two producing wells equidistant from an injection well, as shown in Fig. 1. They used a grid that aligns producer 2 with the injector well, consequently, there is a numerical preferable path for the displacement front. The data can be found in Hegre *et al.* (1986).
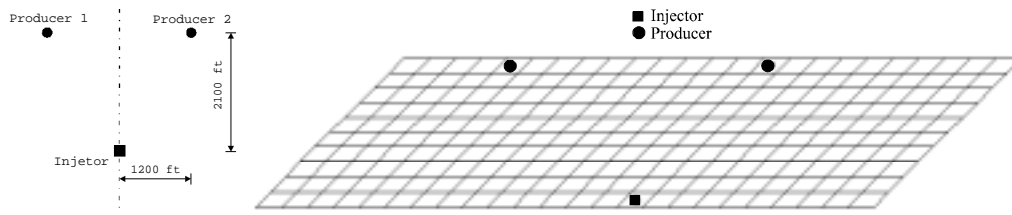
Figure 1 – Well's configuration and the grid used (24x10)

Observing Fig. 2 one can see that UDS introduces excessive numerical diffusion, resulting in a breakthrough difference of more than 800 days. Meanwhile, by applying TVD with 3rd order limit function and ENO two benefits arise. First, the flood front becomes sharper, delaying the breakthrough of the wells and allowing reliable oil recovery analysis. Second, the forecast breakthrough differences decrease. One can note, looking at Table 1, that the use of TVD and ENO, in this case, diminish the breakthrough difference in 42.4 and 22.5 percent, respectively.
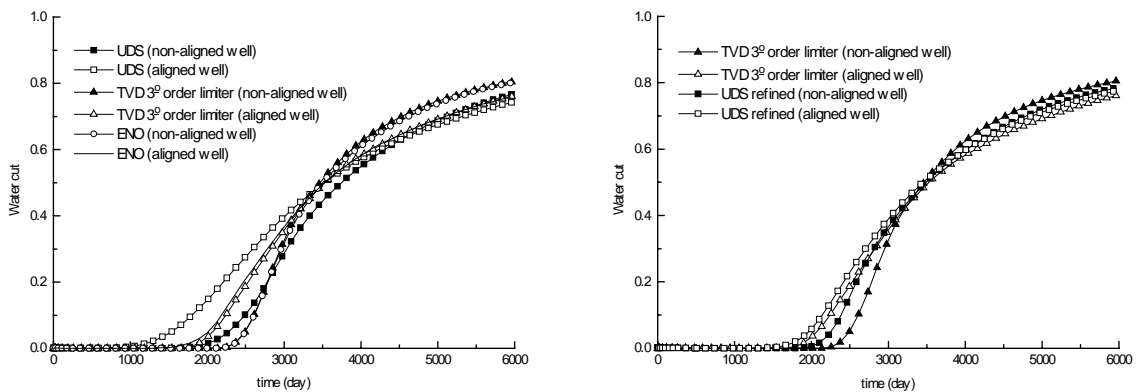
Figure 2 – Water cut results of the three-well system problem

Figure 3 depicts the water saturation map for each scheme for 1000 days. One can observe that the displacement front is better captured using TVD and ENO schemes than UDS, except for the refined UDS. However, in spite of these high-resolution schemes better capture the sharp fronts, it can be seen the existence of a preferable flow path by the distortion of the iso-saturation lines, showing the presence of grid orientation effects. Therefore, Fig. 3 is helpful for understanding that high-resolution schemes do not attack the grid orientation problem working on equalizing the spatial distribution of truncation errors, as is done in nine point schemes, but working on better prediction of the high gradients in the domain. For a

consistent numerical scheme, all errors disappear when the grid is refined and so does the grid orientation effect. For coarse grids, however, the orientation effect can be resolved using two approaches: directly, by the truncation error homogenization, or indirectly, by a more accurate saturation front solution, as done with high-resolution schemes.

Table 1 – Forecast breakthrough for each scheme (values in days)

Scheme (grid)	Non-aligned well	Aligned well	Difference
UDS (24x10)	1931.42	1117.83	813.58
UDS ref. (72x30)	2113.17	1726.47	386.70
TVD 3rd (24x10)	2317.28	1848.64	468.64
ENO (24x10)	2320.06	1689.36	630.70
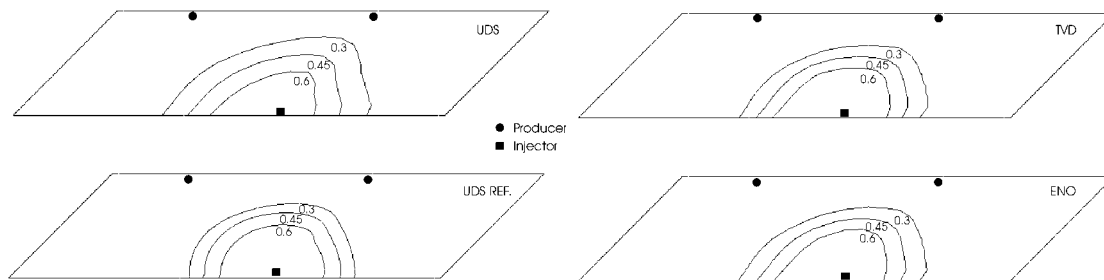
Figure 3 – Saturation maps for 1000 days for the three-well system problem.

6. CONCLUSIONS

This paper presents methods to solve two-phase and three-phase reservoir problems concerning the convective terms approximation. The use of high-resolution schemes is suggested to avoid excessive numerical diffusion. Besides that, this work suggests an ENO scheme to be used in reservoir simulation with boundary fitted-coordinates.

The performance of numerical methods, UDS, TVD and ENO, is analyzed for some reservoir engineering problems using non-orthogonal grids. Comparisons are made with semi-analytical solution and refined grid UDS solutions. The main conclusions are:

- The greatest quality of TVD and ENO schemes is their ability in predicting sharper saturation fronts.
- The TVD and ENO schemes do not resolve the grid orientation effect directly, but these schemes can decrease it by accurate resolution of the fronts.
- The generalized ENO scheme proposed worked well for the case studied.
- The TVD scheme with third-order limit function obtains better solutions than ENO scheme and is easier to implement. Therefore, it is recommended the use of TVD with third-order limit function instead of the ENO scheme.

Acknowledgements

REFERENCES

Bell, J.B. and Shubin, G.R., 1985, Higher-order Godunov methods for reducing numerical dispersion in reservoir simulation, SPE paper 13514.

Chen, W.H., Durlofsky, L.J., Engquist, B. and Osher, S., 1991, Minimization of grid orientation effects through use of higher-order finite difference methods, SPE paper 22887.

Colella, P.; Concus, P. and Sethian, J., 1983, Some numerical methods for discontinuos flows in porous media, pp. 161-186 in The Mathematics of Reservoir Simulation, ed. R. Ewing, SIAM, Philadelphia.

Cunha, A.R., Maliska, C.R., Silva, A.F.C. and Livramento, M.A., 1994, Two-dimensional two-phase petroleum reservoir simulation using boundary-fitted grids, V Encontro Nacional de Ciências Térmicas, São Paulo, pp. 359-362.

Czesnat, A.O., Maliska, C.R., Silva, A.F.C. and Lucianetti, R.M., 1998, Effects of the grid orientation in petroleum reservoir simulation using boundary fitted coordinates, ENCIT 98, Proceedings of 7th Brazilian Congress of Engineering and Thermal Sciences, Brasil, pp. 1007-1012.

Glimm, J. and Lax, P.D., 1970, Decay of solutions of systems of nonlinear hyperbolic conservation laws, Mem. Amer. Math. Soc., n. 101.

Harten, A., 1983, High-resolution schemes for hyperbolic conservation laws, Journal of Computational Physics, vol. 49, pp. 357-393.

Harten, A. and Osher, S., 1987, Uniformly high-order accurate non-oscillatory schemes I, SIAM J. Numer. Anal., vol. 24, pp. 279-309.

Harten, A., Engquist, B., Osher, S. and Chakravarthy, S. R., 1987, Uniformly high-order accurate non-oscillatory schemes III, Journal of Computational Physics, vol. 77, pp. 439-471.

Hegre, T.M., Dalen, V. and Henriquez, A., 1986, Generalized transmissibilities for distorted grids in reservoir simulation, Paper SPE 15622, Proc. SPE 61st Annual Technical Conference and Exhibition, New Orleans.

Maliska, C.R., 1995, Transferência de Calor e Mecânica dos Fluidos Computacional, LTC - Livros Técnicos e Científicos Editora S. A., Rio de Janeiro, RJ, Brasil.

Maliska, C.R., Silva, A.F.C., Czesnat, A.O., Lucianetti, R.M. and Maliska Jr., C.R., 1997, Three-dimensional multiphase flow simulation in petroleum reservoirs using the mass fractions as dependent variables, SPE 39067.

Maliska, C. R., Silva, A. F. C., Jucá, P. C., Cunha, A. R., Livramento, M. A., 1993, Development of a Threee-Dimensional Balck-Oil Simulator Using Boundary-Fitted Coordinates (in portuguese), Part I, Report prepared to: CENPES/PETROBRÁS, , RT-93-1, Florianópolis, SC, Brasil.

Mota, M. A. A. e Maliska, C. R. *"Simulação Numérica de Reservatórios de Petróleo Utilizando Coordenadas Generalizadas e Interpolação TVD"*, Anais V ENCIT, pp. 325-328, São Paulo, Brasil, 1994.

Pinto, A.C.C., Correia, A.C.F. and Cunha, M.C. de CASTRO, 1992, High-resolution schemes for conservation laws: applications to reservoir engineering, SPE paper 24262.

Rubin, B. and Blunt, M. J., 1991, Higher-order implicit flux limiting schemes for Black-Oil simulation, SPE 21222, pp. 219-229, California.

SHU, C.W. and OSHER, S, 1988a, Efficient implementation of essentially non-oscillatory shock-capturing schemes, J. Comp. Phys., vol. 71, pp. 439-471.

_____, 1988b, Efficient implementation of essentially non-oscillatory shock-capturing schemes, II, J. Comp. Phys., vol. 83, pp. 32-78.

Taggart, I.J. and Pinczewski, W.V., 1987, The use of higher order differencing techniques in reservoir simulation, Paper presented at the Sixth SPE Symposium on Reservoir Simulation, Dallas, Texas.

Yanosik, J.L. e McCraken, T.A., 1976, A nine-point, finite-difference reservoir simulator for realistic prediction of adverse mobility ratio displacements, SPE J., pp. 253-262.